

**Trapping in self-avoiding walks with nearest-neighbor attraction**Wyatt Hooper  and Alexander R. Klotz \**Department of Physics and Astronomy, California State University, Long Beach, California 90840, USA*

(Received 24 June 2020; accepted 1 September 2020; published 18 September 2020)

The statistics of self-avoiding random walks have been used to model polymer physics for decades. A self-avoiding walk that grows one step at a time on a lattice will eventually trap itself, which occurs after an average of 71 steps on a square lattice. Here, we consider the effect of nearest-neighbor attractive interactions on isolated growing self-avoiding walks, and we examine the effect that self-attraction has both on the statistics of trapping as well as on chain statistics through the transition between expanded and collapsed walks at the theta point. We find that the trapping length increases exponentially with the nearest-neighbor contact energy, but that there is a local minimum in trapping length for weakly self-attractive walks. While it has been controversial whether growing self-avoiding walks have the same asymptotic behavior as traditional self-avoiding walks, we find that the theta point is not at the same location for growing self-avoiding walks, and that the persistence length converges much more rapidly to a smaller value.

DOI: [10.1103/PhysRevE.102.032132](https://doi.org/10.1103/PhysRevE.102.032132)**I. INTRODUCTION**

A self-avoiding walk (SAW) is a random walk on which no two sites share the same location. In polymer physics, SAWs are used to model excluded-volume repulsion between two segments of a molecule, and the statistics of self-avoiding walks can be used to make measurable predictions about the scaling behavior of polymers and polymer solutions [1]. Typically, the statistics of a self-avoiding walk are averaged over every member of the ensemble that consists of every walk of the same length, assuming that each is equally probable. In contrast, a growing self-avoiding walk (GSAW) on a lattice can be generated by taking a step in a random direction from a lattice site, then a subsequent random step to an open neighboring lattice site, continuing to walk randomly to any unoccupied site until no more sites are available [2]. While every SAW on a specific lattice can in principle be generated as a GSAW, there are two key differences between the GSAW and traditional SAW ensembles, the first being that GSAWs are likely to reach a state where there are no free adjacent sites and the walk becomes “trapped” and terminates [3], and the second that each  $N$ -step walk is not equally likely [2]. It has been debated as to whether the GSAW belongs to the same universality class as the traditional SAW [4].

Trapping is often considered as a bug rather than a feature; various forms of the Rosenbluth method for generating SAW ensembles bias the walk conditions in order to avoid trapping [5]. GSAWs have been proposed as models for polymers whose growth timescales are faster than their relaxation timescales, or more generally as models for polymer growth [6]. Recent investigations into active nematic gels based on microtubule polymerization [7] or so-called “living”

micellar solutions [8] serve as physical examples. A growing self-avoiding walk will inevitably become trapped. This was proven by Hemmer and Hemmer [6], and a simulation of 60 000 GSAWs on a square lattice found that the mean distance reached before trapping was approximately 71 steps, with a probability distribution that peaks near 33 steps. A subsequent thesis by Renner [9] examined trapping in triangular, honeycomb, and simple cubic lattices (among others), and found that the mean length to trapping is approximately 78, 70, and 4000, respectively. The most detailed numerical simulations of GSAW trapping are those of Pfoertner [10], whose simulations are precise enough to identify strong even-odd oscillation in the trapping probability distribution.

In the language of polymer physics, a “good solvent” is one in which excluded volume interactions between distant parts of the chain cause a polymer to adopt a “swollen coil” configuration that is larger than a noninteracting chain of the same length, described by the statistics of a self-avoiding walk. A “poor solvent” is one in which effective attractive interactions between distant parts of the chain dominate over excluded volume interactions and the chain forms a compact “globule” that is smaller than an equivalent length noninteracting chain. The coil-globule phase transition between the two occurs in what is known as a “theta solvent,” in which the attractive and repulsive interactions exactly cancel and the polymer can be described by the statistics of a random walk in three dimensions [11], and three-body interactions become dominant at the theta point in two dimensions [12]. The theta point is a tricritical point [13], in that it not only separates the solvent-rich and polymer-rich states [14], but also delineates between a first- and second-order transition between the two. In practice, the theta point can be found either by fixing the intrachain interaction strength and varying the temperature, or by fixing the temperature and varying the interaction strength with the reciprocal effect. An equivalent transition between swollen and collapsed states may be observed in self-avoiding random

\*alex.klotz@csulb.edu

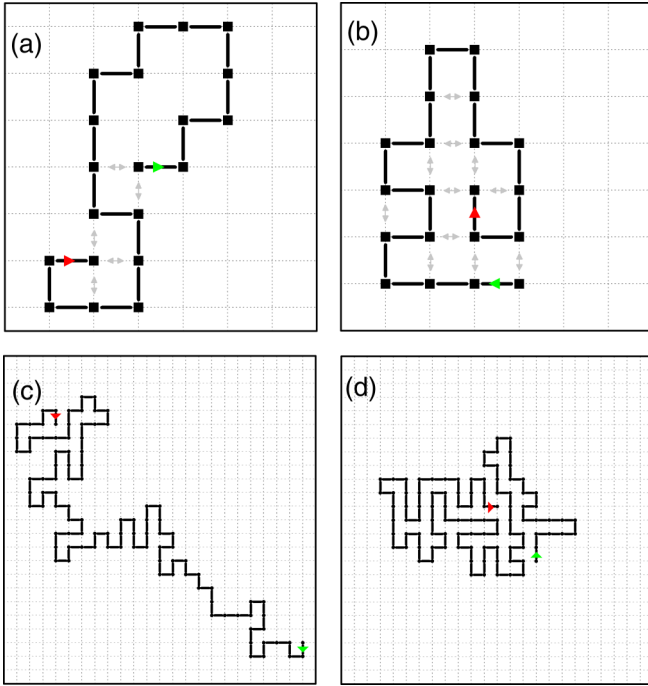


FIG. 1. Diagrams of four trapped walks on a square lattice. The top figures are trapped after 19 steps and the bottom after 99. The left figures were generated at  $\beta\epsilon = 0$  and the right figures at  $\beta\epsilon = 1$ . The first step is indicated with a green arrow, and the final trapped step is indicated with a red arrow. Gray arrows indicate the five nearest-neighbor contacts in (a) and the ten nearest-neighbor contacts in (b).

walks on lattices, where poor-solvent interactions are implemented in terms of an associated energy based on the number of nearest-neighbor contacts between nonadjacent sites on each walk [15]. Exact enumeration [16], Monte Carlo [17], and renormalization-group [18] analysis have identified the theta condition for square lattice SAWs in terms of the critical self-attraction strength and the asymptotic behavior at the transition. While attractive interactions are known to change the asymptotic behavior of self-avoiding walks, and the growing self-avoiding walk has been conjectured to have different behavior from the traditional self-avoiding walk [4,19] (for example, a smaller scaling exponent  $\nu$ ), there has been no examination of the effects of self-attraction on the growing self-avoiding walk. Here, we examine the effect of nearest-neighbor self-attraction on the growing self-avoiding walk in order to ascertain the correlation between trapping statistics and solvent quality and to provide further insight into the differences between the SAW and GSAW ensembles.

## II. THEORY AND SIMULATIONS

A “walk” on a square lattice begins at the site  $\langle 0, 0 \rangle$ . It takes its first step toward any of the  $n = 4$  nearest-neighbor sites with equal probability. For its second step, there are now  $n = 3$  unoccupied adjacent lattice sites. Steps may be taken probabilistically into unoccupied adjacent sites until none remain, at which point the walk is said to have become trapped. The earliest that this can occur is after seven steps. Figure 1

shows examples of walks that have become trapped after 19 and 99 steps.

For a purely self-avoiding walk, the probability of taking a subsequent step to an open lattice site is  $p_o = \frac{1}{n}$ . More generally, each of the  $i = 1, \dots, n$  available steps may be assigned an associated energy  $F$  such that the probability of each step is Boltzmann-weighted by the energy

$$p_i \propto e^{-\beta F_i}. \quad (1)$$

The thermodynamic  $\beta$  is the reciprocal of the thermal energy, equivalent to  $1/T$  in natural units. The probability of each of the  $n$  available steps is

$$p_i = \frac{e^{-\beta F_i}}{\sum_{j=1}^n e^{-\beta F_j}}. \quad (2)$$

In a system with no interactions beyond self-avoidance, the associated energy of each step is zero, the probability of each open step is equal, and Eq. (2) is identical to that of Lyklema and Kremer [19]. The probability of each possible first step on a square lattice is  $1/4$ , and it is  $1/3$ ,  $1/2$ , or  $1$  for each subsequent step depending on the number of empty adjacent sites. The probability of stepping toward an occupied site is always zero, in contrast to the Domb-Joyce model [20] in which an energetic cost is given to multiply-occupied sites, or the self-avoiding trail model in which only lattice sites but not edges may be shared [21].

To study the effects analogous to those experienced between nonadjacent monomers in a polymer chain in a poor solvent, we include a negative energy associated with nearest-neighbor contacts between nonadjacent sites [indicated with gray arrows in Figs. 1(a) and 1(b)]. Such a model is typically used when discussing the theta-point transition in lattice walks. The energy of each walk in the ensemble depends favorably on the total number  $m$  of nonadjacent occupied nearest-neighbor lattice sites, with interaction energy  $\epsilon$  per pair:

$$F_i = -\epsilon m. \quad (3)$$

The Boltzmann-weighted probability of each state is

$$p_i = \frac{e^{\beta \epsilon m_i}}{\sum_{j=1}^n e^{\beta \epsilon m_j}}. \quad (4)$$

In simulations parametrized to physical polymers, poor-solvent behavior corresponds roughly to values of  $\beta\epsilon$  above  $0.5$  [22]. In the GSAW ensemble, the number of *new* nearest-neighbor contacts arising from a step will be between  $0$  and  $3$ . Since each possible state shares a common “history,” the number of contacts in the  $(N - 1)$ th step need not be recomputed. For example, the final step in Fig. 1(a) gains three new nearest-neighbor contacts. If the last step had been up instead of right, it would have gained one new contact, and zero if it had been to the left. Counting every step, rather than just new steps, the choices would be between two, three, and five steps. Computing the probability of a given step in the above situation using Eq. (4) acquires a factor of  $\exp(2\beta\epsilon)$  in both the numerator and denominator if total steps (rather than new steps) are taken into account, which have no net effect. For computational ease, the probabilities need only be computed based on the number of new contacts in each potential step. In

all nontrapped walks, the probability of each allowable step sums to unity. In the above example, the total probability is

$$p_t = \frac{1}{1 + e^{\beta\epsilon} + e^{3\beta\epsilon}} + \frac{e^{\beta\epsilon}}{1 + e^{\beta\epsilon} + e^{3\beta\epsilon}} + \frac{e^{3\beta\epsilon}}{1 + e^{\beta\epsilon} + e^{3\beta\epsilon}} = 1. \quad (5)$$

Growing self-avoiding walks were simulated with MATLAB using parallel CPU computation. The uniform random number generation in MATLAB is based on the Mersenne Twister [23]. Walks were simulated for  $\beta\epsilon$  from 0 to 0.6 in increments of 0.01, and up to 3.3 in increments of 0.1. At least 75 000 walks were generated for each value of  $\epsilon$ , with additional walks generated for specific values of interest. 1.25 million were generated for the  $\epsilon = 0$  case. For  $\beta\epsilon$  values of 6 and 10, 100 000 walks of maximum length 600 were generated to study chain statistics, but it was computationally unfeasible to study trapping at large  $\epsilon$ .

### III. RESULTS AND DISCUSSION: TRAPPING

There are several metrics that can characterize the characteristic length of a self-trapping walk, including the mean, median, and peak of the probability distribution. Here, we will primarily discuss the mean trapping length and its dependence on the nearest-neighbor attraction strength. Other metrics of the trapping distribution are presented in the Appendix.

In the simple case of zero self-attraction, we find that the mean trapping length is  $70.85 \pm 0.05$ , consistent with the findings of Hemmer and Hemmer [3], and within two standard errors of the computations from Pfoertner [10]. The findings from Renner [9] are approximately 1.0 greater than those of Hemmer, Pfoertner, and the present work, suggesting a node-versus-step discrepancy.

Trapping requires that the walk first creates a void bounded by occupied sites, and then walks into the void. Voids are unlikely to form in the limit of strong self-attraction, so it may be expected that the mean trapping length increases with the attraction strength. Indeed, we do observe an exponential increase in the mean trapping length with respect to  $\epsilon$  [Fig. 1(a)]. For  $\beta\epsilon > 1$ , the mean trapping length increases exponentially, approximately described by the function  $\langle N \rangle \propto e^{1.12\beta\epsilon}$ . The largest value of  $\beta\epsilon$  for which we measured full trapping statistics was 3.3, at which the mean trapping length was 1152. In 100 000 runs up to length 600, only 120 walks became trapped at  $\beta\epsilon = 6$  (the lowest at 77 steps), and no trapping events were observed at  $\beta\epsilon = 10$ .

Notably, there is a local minimum at approximately  $\epsilon = 0.28$  at which the mean trapping length is 67.2 [Fig. 2(b)]. While counterintuitive, the local minimum may be understood by considering that a walk entering a previously formed void will likely have more nearest-neighbor contacts than if it were to avoid the void. When self-attraction is strong, voids are less likely to form for walks to become trapped, but when self-attraction is weak, there is no bias to walk into the voids that do form. The local minimum in the trapping length arises when there is sufficient self-attraction to bias the walks into voids, without suppressing their formation altogether.

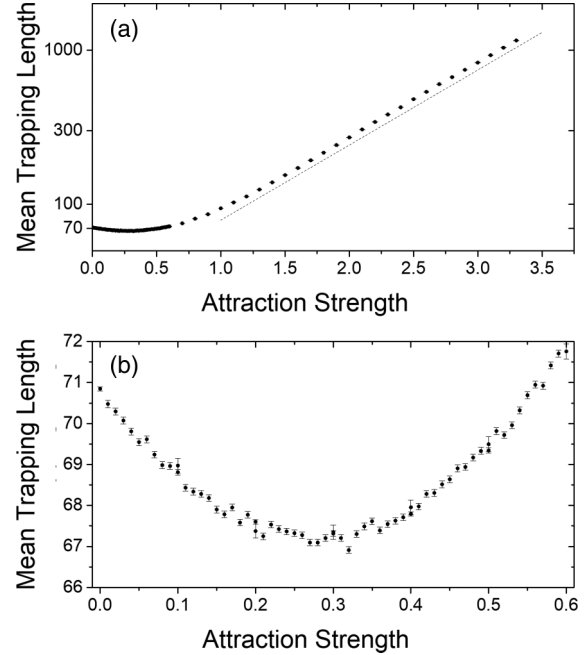


FIG. 2. (a) Mean trapping length of growing self-avoiding walks as a function of the nearest-neighbor self-attraction strength. The dashed line shows an exponential function with a best-fit coefficient of 1.12. (b) The local minimum in trapping length with respect to attraction strength. The minimum is at approximately  $\beta\epsilon = 0.28$  and  $\langle N \rangle = 67.2$ .

To further understand the local minimum in the mean trapping length, we can consider the shortest trapped state as an example, which can occur after seven steps. To become trapped after seven steps [Fig. 3(a)], the third and fifth step must both be in an unfavored direction in order to open a void, while the final step must be the most favored step into the void. The exact probability of trapping after seven steps can be calculated from the product of the probability of each necessary step:

$$P_7 = \frac{2}{27} \frac{e^{3\beta\epsilon}}{(2 + e^{\beta\epsilon})(2 + e^{2\beta\epsilon})(1 + e^{\beta\epsilon} + e^{3\beta\epsilon})}. \quad (6)$$

This is derived in further detail in the Appendix. The minimal trapping probability is nonmonotonic with respect to the attraction strength, with a local maximum at approximately 0.234. The minimal trapping probability is well-described by numerical data [Fig. 3(b)]. The maximum in the  $N = 7$  trapping probability is analogous to the minimum in the mean trapping length. In principle, one could calculate exact probabilities for longer trapped states and derive the mean trapping length  $7P_7 + 8P_8 + 9P_9 \dots$ , but this becomes difficult as the number of possibilities increases. The minimal trapping probability for the triangular and honeycomb lattices can also be derived, showing that the same local maximum exists in the triangular lattice, but not the honeycomb.

The distribution of trapping lengths was previously described by Hemmer and Hemmer [3] as power-law growth below the peak and exponential decay beyond the peak, finding that for  $\epsilon = 0$ ,  $p(N) \approx (N - 6)^{3/5} e^{-N/40}$ . Renner [9] described similar behavior with a more complex function. We

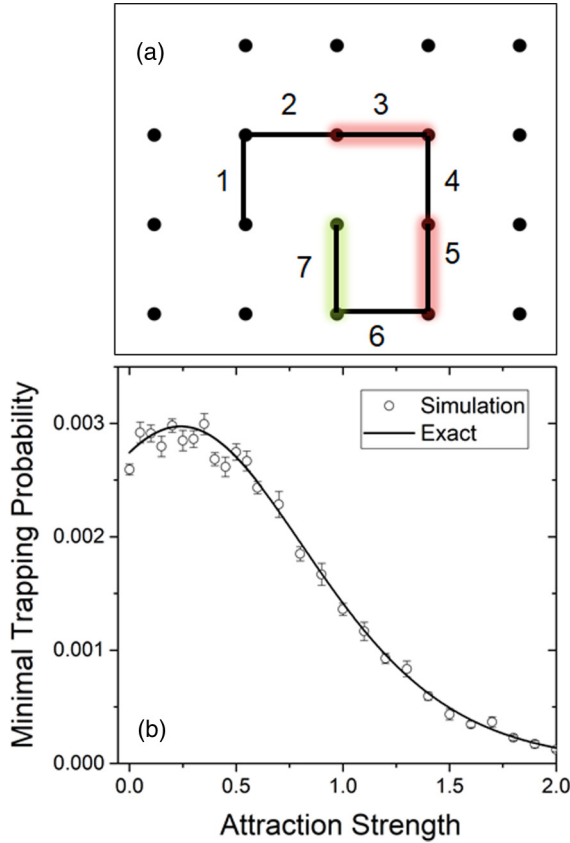


FIG. 3. The shortest self-trapping walk lasts seven steps. (a) An example of a minimally trapped walk. Red lines highlight steps necessary for minimal trapping, which are unfavorable because they are not in the direction that increases the number of nearest-neighbor contacts. The final step, highlighted in green, leads to trapping and maximizes the number of nearest-neighbor contacts. (b) Calculated probability of trapping after seven steps, according to Eq. (6), overlaid with simulation results.

may examine histograms of trapping probability at various  $\epsilon$  and see that the peaks are indeed shifted to the right and the tails become broader with increasing  $\beta\epsilon$ . We can, in principle, make similar fits to histograms and examine how the fit parameters depend on  $\epsilon$ . The trapping probability is however not characterized by a single distribution, but two. Even-odd oscillation in the trapping probabilities has been observed for  $\epsilon = 0$ , with odd-valued trapping being slightly more likely (for example, the probability of trapping after eight steps is  $5/6$  that of seven steps). This can be explained by the abundance of trapped SAWs of various lengths, which itself has even-odd dependence [10]. The asymmetry becomes more pronounced with increasing  $\beta\epsilon$ , where histograms curves corresponding to each parity are clearly distinct (Fig. 4). The probability of trapping in an even state decreases continuously with  $\beta\epsilon$ , but the distribution of even trapping lengths is typically longer than that of odd: the ratio of the mean of the odd-length to even-length walks reaches a plateau of about 1.05 (Fig. 5). It may be conjectured that the parity asymmetry is an artefact of the square lattice. We also note that the nonmonotonic trend in the trapping probability with respect to the attraction strength is not present in the parity asymmetry.

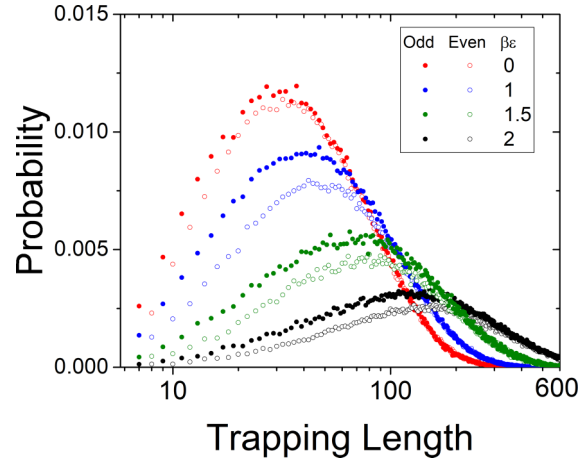


FIG. 4. Probability distribution of trapping lengths at  $\beta\epsilon$  values of 0, 1, 1.5, and 2. Odd trapping lengths are indicated with solid symbols and even trapping lengths with open symbols. There is strong parity oscillation, which is heightened with increasing self-attraction.

IV. RESULTS AND DISCUSSION: CHAIN STATISTICS

While the primary aim of this study was to examine the effect of self-attraction on self-trapping, we may also examine the statistics of the growing self-avoiding walk ensemble in comparison to traditional self-avoiding walks. We preface this by noting that attrition due to self-trapping leads to significantly reduced samples of large walks, which are most important for evaluating critical behavior.

The metric we use to discuss chain statistics is the radius of gyration,  $R_g$ , which is the standard deviation of the position of every node in the walk, relative to the center-of-mass position. It may be compared to the end-to-end distance,  $R_{ee}$ , which is the Pythagorean distance between the origin and the  $N$ th site. Both the end-to-end distance and the radius of gyration are expected to scale according to a power law with respect to  $N$  for sufficiently long walks, described by an exponent  $\nu$ , referred to as the scaling exponent.

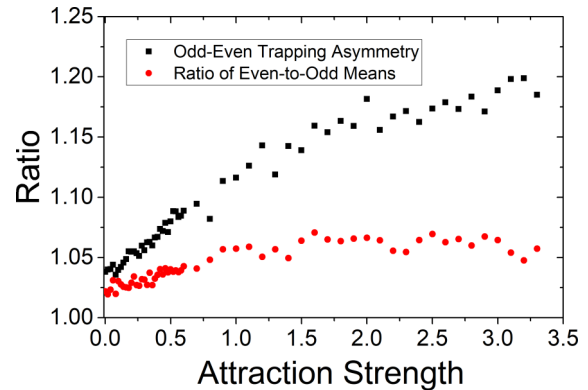


FIG. 5. Parity asymmetry as a function of increased attraction strength. Black points indicate the ratio of odd-length trapped walks to even-length trapped walks, which increases continuously. Red points indicate the ratio of the means of the even-length population to the odd-length population, which approaches a plateau near 1.05.

For traditional SAWs in two dimensions, the “good solvent” scaling exponent is 0.75, known as the Flory exponent. For collapsed chains, because the area of a walk is proportional to its length, the exponent is expected to be 0.5. For asymptotically long chains, the exponent is 0.75 at any temperature above the theta point and 0.5 at any temperature below it, with a transition at which the exponent is  $4/7 \approx 0.57$ . For finitely long chains, there is a smooth transition from 0.75 through  $4/7$  toward 0.5 [24].

There has been uncertainty in the literature over whether the GSAW follows the same asymptotic behavior as the traditional SAW with regard to its universal exponents. Initially the exponent  $\nu$  was determined by Majid *et al.* [4] to be 0.66, followed by Lyklema and Kremer [19], who estimated 0.68; both are below the Flory value of 0.75. Subsequently, Lyklema and Kremer argued that the exponent  $\nu$  would approach the Flory value for walks that were of such great lengths that the convergence [would likely never be seen via simulation] [2].

To understand why the GSAW may be asymptotically smaller than the SAW, consider the probability of finding a walk extended along a straight line. For the GSAW, the first step may be taken in any direction, and each subsequent step has a  $1/3$  probability of remaining straight. The probability of finding a length- $N$  GSAW in a straight line is thus  $(1/3)^{N-1}$ . For a SAW of length  $N$ , there are four extended walks, and asymptotically  $\sim 2.64^N$  total walks [25], meaning the probability of finding a straight path is  $4/2.64^N$ . It is asymptotically much more likely to find an extended SAW than an extended GSAW, and it can be argued that ensemble-averaged GSAWs are asymptotically smaller than SAWs.

While we cannot answer the question of asymptotic scaling in the affirmative or negative, we can examine the effect of self-attraction on GSAW statistics in order to identify the swollen-collapsed transition at the theta point. For a square lattice SAW with nearest-neighbor attraction in two dimensions, the transition occurs at  $\beta\epsilon \approx 0.66$  with a scaling exponent of  $4/7$  [26].

The scaling of the mean radius of gyration as a function of walk length for several values of  $\epsilon$  may be seen in Fig. 6(a). Generally, the radius scales as a power law, with the exponent decreasing with increasing self-attraction. For  $\epsilon = 0$ , the scaling is similar to the 0.68 seen by Lyklema and Kremer [19], while for large  $\beta\epsilon$  it approaches the 0.5 expected in the compact state. We note that for large  $\epsilon$ , the behavior of a growing walk is essentially that of an expanding spiral, and many of the traits of an ensemble of “random” walks are no longer seen.

Figure 6(b) shows the results of least-squares power-law fits to various parts of the  $R_g$ -vs- $N$  data. As expected, there is a smooth transition with  $\epsilon$  from between 0.65 and 70 at  $\epsilon = 0$  to a collapsed state near 0.5 for large  $\beta\epsilon$ . The transition is sharper when the fit is made with larger values of  $N$ , but there is no definitive evidence of a first-order transition between coil-like and globule-like phases [13,14].

One means of identifying the theta point is to find the value of the attraction strength for which length dependence vanishes. While the curves appear to converge near  $\beta\epsilon = 3$ , they do not meet at a single point. Rather, the intersection between two  $\nu$ - $\epsilon$  curves tends to move toward larger  $\epsilon$  with increasing length. We note that the traditional SAW  $\theta$  point,

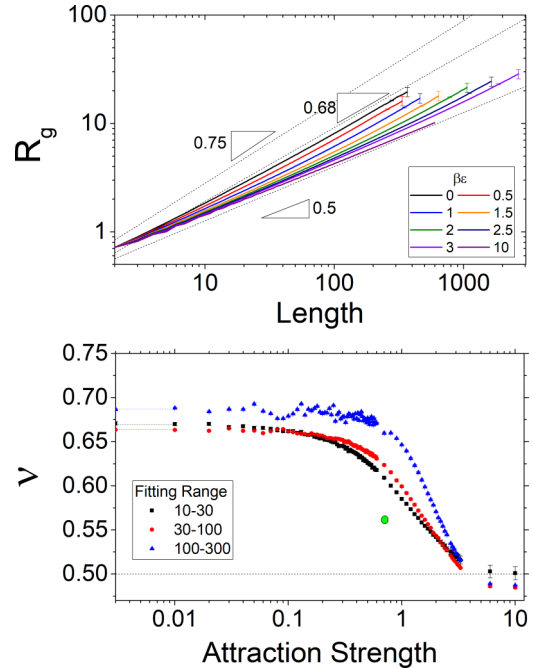


FIG. 6. (a) Mean radius of gyration of the ensemble on logarithmic axes at  $\beta\epsilon$  values of 0, 0.5, 1, 1.5, 2, 2.5, 3, and 10. Data were included until the standard error exceeded 10%. For clarity, error bars are only shown on the final point, which are at lengths of 367, 334, 459, 639, 1063, 1638, 2660, and 600 in order of increasing  $\beta\epsilon$ . For comparison, power-law curves are shown for the 2D Flory exponent (0.75), the expectation for the collapsed phase (0.5), and the value ascertained by Lyklema and Kremer (0.68) [19]. (b) Best-fit length scaling exponent of  $R_g$ , plotted as a function of the attraction strength. The fits were taken at lengths 10–30, 30–100, and 100–300. The green circle represents the  $\theta$  condition for standard self-avoiding walks.  $\epsilon = 0$  values that would otherwise be absent on a logarithmic axis are shown on the y axis with horizontal lines.

at  $\beta\epsilon = 0.66$  and  $\nu = 4/7$ , is entirely inconsistent with the GSAW data, and we expect from Fig. 6(b) that more data at increased lengths would push the transition toward even larger  $\epsilon$ . We present additional data to support this in the Appendix. Although we have not uniquely identified the  $\theta$  point for the GSAW, we can conclusively refute the hypothesis that the critical value of  $\beta\epsilon$  is the same as the SAW.

Another metric we can examine is the ratio between the squares of the radius of gyration to the end-to-end distance, also known as a universal amplitude ratio. This ratio reaches a universal constant for asymptotically long polymers, which is approximately 0.18 at the theta point for square lattice walks [26]. In the swollen regime, the ratio is approached from below with respect to length, while in the collapsed regime it is approached from above, and the ratio is approximately independent of length at the theta point [5]. Examining the data in Fig. 7(a), it can be seen that the ratio increases with small  $N$  for values of  $\beta\epsilon$  above 1.5 and decreases below it. For any value of  $\beta\epsilon$ , however, there is a length beyond which the ratio begins to decrease such that no value of  $\epsilon$  will produce a horizontal curve. Figure 7(b) shows the ratio at several lengths as a function of the attraction strength with a similar trend to the scaling exponent data in that there is

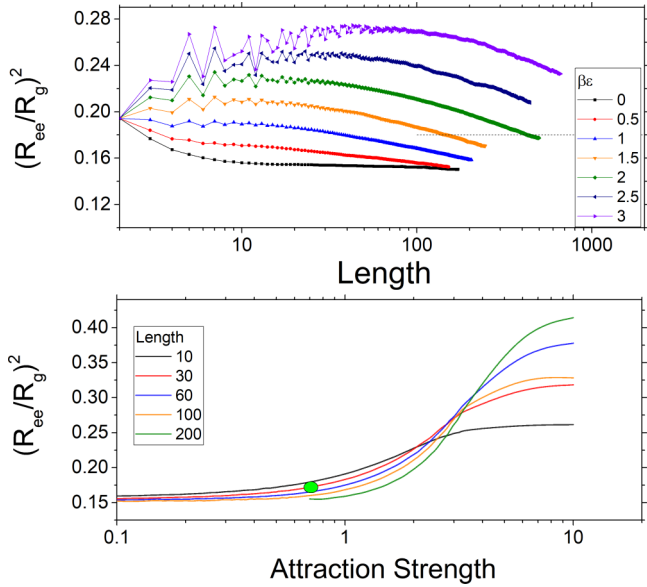


FIG. 7. (a) Universal amplitude ratio of the squares of the radius of gyration  $R_g$  and end-to-end distance  $R_{ee}$  as a function of chain length for several values of attraction strength. The dashed horizontal line represents the value for the SAW theta condition. (b) The same ratio plot as a function of the attraction strength for several lengths. The scarce data for small  $\beta\epsilon$  at  $N = 200$  are not shown. The green circle represents the theta point for SAWs.

minimal but nonzero length dependence around  $\beta\epsilon = 3$ , but it moves toward greater  $\epsilon$  with increasing length. Similar to the scaling exponent data, there is no single value of  $\beta\epsilon$  for which the universal amplitude ratio converges independently of length, and to the extent that there is convergence, it is not at the SAW value of either  $\beta\epsilon$  or  $R_g^2/R_{ee}^2$ .

A final parameter of interest is the persistence length of the walk, sometimes known as the “persistency” to distinguish it from the persistence length of the wormlike chain. The persistence length of a self-avoiding walk represents the “memory” a walk has for the direction of its first step. It is defined by Grassberger [27] over an ensemble of walks of length  $N$  as the mean coordinate of the  $N$ th step in the direction of the first step, or equivalently the dot product of the position vector of the  $N$ th step and the first step.

Based on enumerations of self-avoiding walks on the square lattice, Grassberger concluded that the persistence length diverged with a 0.06 power law dependence on length [27]. Redner [29] argued using the same data that the persistence was logarithmically divergent, rather than obeying a power law. Eisenberg [30] later used Monte Carlo techniques and examined angular correlation functions to argue that they decayed in such a way as to imply a finite persistence length. Granzotti *et al.* recently extended Eisenberg’s result to state that the persistence length was in fact 2.66 [28].

Figure 8(a) shows the persistence as a function of length for four values of  $\epsilon$ . In general, the persistence converges beyond 10 or 20 steps, with noticeable even-odd effects. The convergent value typically decreases with increasing attraction strength. For the  $\epsilon = 0$  case, the persistence converges to approximately  $1.402 \pm 0.001$ . It is tantalizing but unjustified

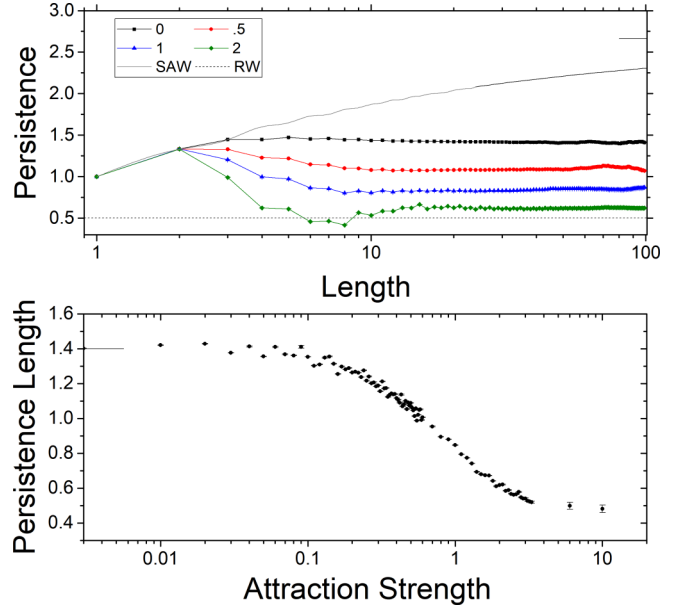


FIG. 8. (a) The persistence, defined as the mean position of the  $N$ th step in the direction of the first step, as a function of walk length for several values of the attraction strength. The persistence has a convergent value that decreases with attraction strength. For comparison, the random-walk value of 0.5 and the values for the traditional self-avoiding walk [28] and its asymptotic value of 2.66 are shown. (b) Persistence length as measured by the mean value from length 30 to 60, as a function of attraction strength.

to ascribe the square root of 2 to this value. Figure 8(b) shows the persistence length as a function of attraction strength, which decreases smoothly from 1.4 toward approximately 0.5. Compared to the ongoing controversy over the convergence of the SAW persistence, as well as to finite-length effects in other metrics, it is quite clear that the GSAW persistence converges.

## V. CONCLUSION

Including nearest-neighbor attraction in the growing self-avoiding walk tends to increase the average number of steps before trapping. However, a local minimum in the trapping length arises for weak values of self-attraction. This can be understood from the idea that a walk must both open a void and step into it in order to become trapped; strongly self-attractive walks do not open voids, while weakly self-attractive walks will not necessarily step into them. Investigating the chain statistics of the GSAW ensemble in comparison to the traditional SAW, we have shown that the theta point, if it exists, does not occur at the same value of  $\epsilon$ , and that the persistence length is convergent and approximately half that of the SAW. Many of the effects seen in the limit of strong attraction manifest themselves as odd-even effects that may be artefacts of the square lattice and include only nearest-neighbor interactions. Broadening the analysis to other lattices and including next-nearest-neighbor interactions would be a worthwhile future investigation. It may be asked whether there is a correlation between trapping statistics and chain statistics, in the same way that the growth of SAW enumerations shares a parameter with its metric scaling [31]. This is not manifestly the case,

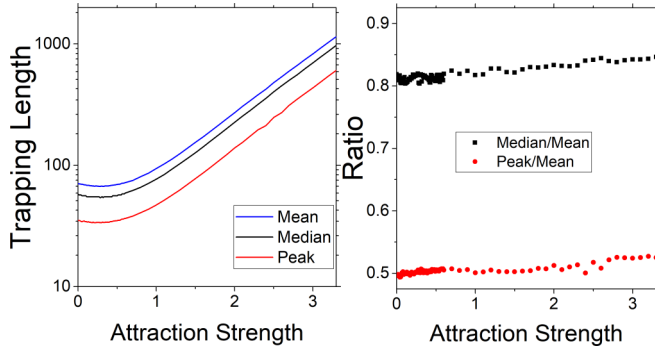


FIG. 9. (a) Mean, median, and distribution peak of the trapping length as a function of the attraction strength. (b) Ratio of the median and the peak to the mean trapping length as a function of the attraction strength.

as the most interesting feature of the trapping statistics occurs at  $\beta\epsilon \approx 0.25$ , and the most interesting feature of the chain statistics occurs at  $\beta\epsilon \approx 3$ . We hope that this work encourages more computationally sophisticated investigations into the GSAW chain and trapping statistics.

#### ACKNOWLEDGMENTS

The authors are grateful to Beatrice W. Soh, Galen Pickett, Douglas R. Tree, Yuri Kopylovski, Kurt Kremer, and Hugo Pfoertner for helpful discussions. W.H. is supported by the CSULB Undergraduate Research Opportunity Program.

#### APPENDIX

##### 1. Alternative trapping metrics

Figure 9(a) shows the median and distribution peak of the trapping length as a function of the attraction strength alongside the mean. The peak of the distribution is found based on a fit to each trapping histogram using Hemmer and Hemmer's power-exponential function [3]. This measurement is less noisy than the mode of the distribution, but it may slightly overpredict the location of the peak (within one step length), in addition to ignoring parity effects. Figure 9(b) shows the ratio of the median and peak to the mean, both of which increase weakly with the attraction strength.

##### 2. Minimal trapping probability

Consider the seven labeled steps in Fig. 3(a). There are eight possible configurations, with fourfold rotational symmetry on the first step and twofold reflection symmetry on the second step. We will consider the probability that each of the first seven steps of a walk will be the step required for minimal trapping. The first step may be taken in any direction,

$$p_1 = 4\frac{1}{4}.$$

The second step may be taken in any of three directions, two of which lead to trapping,

$$p_2 = 2\frac{1}{3}.$$

Assuming without loss of generality that the first two steps are in the  $+y$  and  $+x$  direction as in Fig. 3(a), if the third

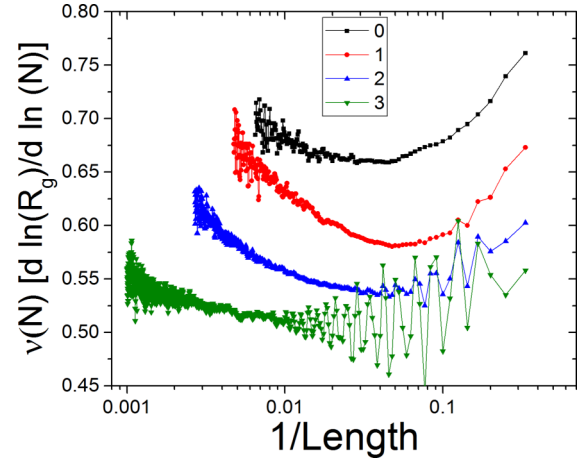


FIG. 10. Local scaling exponent of the radius of gyration for several values of  $\beta\epsilon$ , plot against the reciprocal of the walk length.

step is taken in the  $-y$  direction it will increase the number of neighbor contacts by 1. The probability of the necessary third step is

$$p_3 = \frac{1}{2 + e^{\beta\epsilon}} \leq \frac{1}{3}.$$

The fourth step cannot change the number of contacts,

$$p_4 = \frac{1}{3}.$$

The fifth step is similar to the third in that it must avoid increasing the number of contacts by 2,

$$p_5 = \frac{1}{2 + e^{2\beta\epsilon}} \leq \frac{1}{3}.$$

The sixth step cannot change the number of contacts,

$$p_6 = \frac{1}{3}.$$

Finally, the seventh step must be in the  $+y$  direction to increase the number of contacts by 3 in order to become trapped. An alternative step in the  $-x$  direction would increase the number of contacts by 1, and a step in the  $-y$  direction would leave it unchanged:

$$p_7 = \frac{e^{3\beta\epsilon}}{1 + e^{\beta\epsilon} + e^{3\beta\epsilon}} \geq \frac{1}{3}.$$

The product of each of these probabilities is the total probability of becoming trapped after seven steps, as outlined in Eq. (6) and plotted in Fig. 3(b). There are two nondegenerate eight-step trapped walks, the probabilities of which are left as an exercise for the reader.

##### 3. Length dependence of scaling exponents

Figure 6(b) shows the best-fit scaling exponents at various lengths. Following the conventions of Lyklema and Kremer [19] and others, we can define the "local" scaling exponent for walks of a given length as

$$\nu(N) = \frac{\ln(R_g(N+1)) - \ln(R_g(N-1))}{\ln(N+1) - \ln(N-1)}.$$

Figure 10 shows the local scaling exponent at various values of  $\beta\epsilon$  as a function of reciprocal length, such that its behavior may be extrapolated toward asymptotically long chains. The data are truncated when they become excessively noisy. Each curve starts at small  $N$  at a local maximum (the “rodlike” limit), reaches a global minimum, and then approaches its asymptotic limit as  $(1/N)$  approaches 0. The second conclusion of Lyklema and Kremer [2] is that the asymptotic limit

of the  $\epsilon = 0$  data is 0.75, which we cannot support or refute with our current data. The jagged behavior of the  $\beta\epsilon = 3$  data is a lattice-induced parity effect. Although each set of data approaches its asymptotic limit from below, if there is a discrete transition at a theta point for which there is minimal length dependence, we might expect data beyond that point to approach the limit from above [32], which is not observed.

- 
- [1] D. S. McKenzie and M. A. Moore, Shape of self-avoiding walk or polymer chain, *J. Phys. A* **4**, L82 (1971).
- [2] J. W. Lyklema and K. Kremer, Monte carlo series analysis of irreversible self-avoiding walks. ii. the growing self-avoiding walk, *J. Phys. A* **19**, 279 (1986).
- [3] S. Hemmer and P. C. Hemmer, An average self-avoiding random walk on the square lattice lasts 71 steps, *J. Chem. Phys.* **81**, 584 (1984).
- [4] I. Majid, N. Jan, A. Coniglio, and H. E. Stanley, Kinetic Growth Walk: A New Model for Linear Polymers, *Phys. Rev. Lett.* **52**, 1257 (1984).
- [5] P. Grassberger, Pruned-enriched Rosenbluth method: Simulations of  $\theta$  polymers of chain length up to 1 000 000, *Phys. Rev. E* **56**, 3682 (1997).
- [6] P. C. Hemmer and S. Hemmer, Trapping of genuine self-avoiding walks, *Phys. Rev. A* **34**, 3304 (1986).
- [7] S. J. DeCamp, G. S. Redner, A. Baskaran, M. F. Hagan, and Z. Dogic, Orientational order of motile defects in active nematics, *Nat. Mater.* **14**, 1110 (2015).
- [8] A. V. Korobko and N. A. M. Besseling, Near-second-order transition in confined living-polymer solutions, *Phys. Rev. E* **93**, 032507 (2016).
- [9] A. Renner, E. Bornberg-Bauer, I. L. Hofacker, P. K. Schuster, and P. F. Stadler, Self-avoiding walk models for non-random heteropolymers, Thesis, University of Vienna, 1996.
- [10] H. Pfoertner, Self trapping random walks, <http://www.randomwalk.de/index.html>, Accessed: 2020-06-9.
- [11] A. Pelissetto and J.-P. Hansen, Corrections to scaling and crossover from good-to  $\theta$ -solvent regimes of interacting polymers, *J. Chem. Phys.* **122**, 134904 (2005).
- [12] P.-G. De Gennes and P.-G. Gennes, *Scaling Concepts in Polymer Physics* (Cornell University Press, Ithaca, NY, 1979).
- [13] P. D. Gujrati, Polydisperse solution of randomly branched homopolymers, inversion symmetry and critical and theta states, *J. Chem. Phys.* **108**, 5089 (1998).
- [14] P. D. Gujrati, A binary mixture of monodisperse polymers of fixed architectures, and the critical and the theta states, *J. Chem. Phys.* **108**, 5104 (1998).
- [15] I. Chang and H. Meirovitch, Surface Critical Exponents of Self-Avoiding Walks and Trails on a Square Lattice: The Universality Classes of the  $\theta$  and  $\theta'$  points, *Phys. Rev. Lett.* **69**, 2232 (1992).
- [16] T. Ishinabe, Examination of the theta-point from exact enumeration of self-avoiding walks, *J. Phys. A* **18**, 3181 (1985).
- [17] H. Meirovitch and H. A. Lim, The collapse transition of self-avoiding walks on a square lattice: A computer simulation study, *J. Chem. Phys.* **91**, 2544 (1989).
- [18] F. Seno and A. L. Stella,  $\theta$  point of a linear polymer in 2 dimensions: a renormalization group analysis of monte carlo enumerations, *J. Phys.* **49**, 739 (1988).
- [19] J. W. Lyklema and K. Kremer, The growing self avoiding walk, *J. Phys. A* **17**, L691 (1984).
- [20] A. J. Barrett, On the domb-joyce model for self-avoiding walks in the continuum, *J. Stat. Phys.* **58**, 617 (1990).
- [21] J. W. Lyklema, The growing self-avoiding trail, *J. Phys. A* **18**, L617 (1985).
- [22] L. S. Pam, L. L. Spell, and J. T Kindt, Simulation and theory of flexible equilibrium polymers under poor solvent conditions, *J. Chem. Phys.* **126**, 134906 (2007).
- [23] C. B. Moler, *Numerical Computing with MATLAB* (SIAM, Philadelphia, 2004).
- [24] A. L. Owczarek, T. Prellberg, D. Bennett-Wood, and A. J. Guttmann, Universal distance ratios for interacting two-dimensional polymers, *J. Phys. A* **27**, L919 (1994).
- [25] G. R. Grimmett and Z. Li, Self-avoiding walks and connective constants, in *Sojourns in Probability Theory and Statistical Physics-III* (Springer, Cham, Switzerland, 2019), pp. 215–241.
- [26] S. Caracciolo, M. Gherardi, M. Papinutto, and A. Pelissetto, Geometrical properties of two-dimensional interacting self-avoiding walks at the  $\theta$ -point, *J. Phys. A* **44**, 115004 (2011).
- [27] P. Grassberger, On persistency in self-avoiding random walks, *Phys. Lett. A* **89**, 381 (1982).
- [28] C. R. F. Granzotti, A. S. Martinez, and M. A. A. da Silva, Scaling analysis of random walks with persistence lengths: Application to self-avoiding walks, *Phys. Rev. E* **93**, 052116 (2016).
- [29] S. Redner and V. Privman, Persistency of two-dimensional self-avoiding walks, *J. Phys. A* **20**, L857 (1987).
- [30] E. Eisenberg and A. Baram, The persistence length of two-dimensional self-avoiding random walks, *J. Phys. A* **36**, L121 (2003).
- [31] G. Slade, The self-avoiding walk: A brief survey, *Surv. Stoch. Proc.* **4**, 181 (2011).
- [32] N. R. Beaton, A. J. Guttmann, and I. Jensen, Two-dimensional interacting self-avoiding walks: new estimates for critical temperatures and exponents, *J. Phys. A* **53**, 165002 (2020).